Journal of Catalysis 259 (2008) 54–65

Contents lists available at ScienceDirect

Journal of Catalysis

www.elsevier.com/locate/jcat

A new improvement of catalysis by solid-state electrochemistry: An electrochemically assisted NO_x storage/reduction catalyst

Antonio de Lucas-Consuegra, Ángel Caravaca, Paula Sánchez, Fernando Dorado, José L. Valverde *

Departamento de Ingeniería Química, Facultad de Ciencias Químicas, Universidad de Castilla-La Mancha, Avenida Camilo José Cela 10, 13005 Ciudad Real, Spain

ARTICLE INFO

Article history:
Received 19 May 2008
Revised 10 July 2008
Accepted 22 July 2008
Available online 15 August 2008

Keywords:
Electrochemical catalyst
Electrochemical trapping
Electrochemical regeneration
NO_x storage
NO_x reduction
NSR
Electrochemical promotion
NEMCA effect
Platinum
Potassium

ABSTRACT

In this paper, we report a novel electrochemically assisted NO_x storage/reduction catalyst (Pt–KβAl_2O_3) that can operate over a range of reaction conditions for the effective removal of NO_x. Under negative polarization, NO_x was stored on the catalyst surface in form of potassium nitrates. Under positive polarization, the catalyst was regenerated, and the stored nitrates were efficiently desorbed and reduced to N_2. The variation of the current under the applied polarizations allowed monitoring the progress of both the storing and the regeneration phases, and thus optimisation of the duration of both sequences in a technically feasible manner. In addition, the possibility of electrochemical regeneration of the catalyst surface allowed work under a fixed lean gas composition, which implies an important technological advance for the NSR process. The electrochemically assisted NO_x storage/reduction experiments were supported by NO_x-TPD and cyclic voltammetry measurements, which also revealed useful information about the chemisorption properties of the electrochemical catalyst.

1. Introduction

The effective control of hazardous nitrogen oxides (NO_x) emitted from diesel and lean-burn engine exhaust has attracted a worldwide attention in recent years as an urgent environmental issue [1,2]. Although three-way catalysts have been optimized to reduce NO_x emissions in rich-burn exhaust, as from consumer automobiles, these catalysts are ineffective under lean-burn conditions, as encountered in stationary sources and diesel engines. Recently, the selective catalytic reduction (SCR) of NO_x, has been proposed as a possible solution to this problem. This process is already widely used for stationary NO_x sources, but would require on-board storage and periodic replenishing of the reducing agent (urea or ammonia) or sacrifice of a portion of the fuel if hydrocarbons used as the reducing agent [3]. A promising alternative for the removal of NO_x under lean-burn conditions is the NO_x storage-reduction catalyst (NSR catalyst), which does not require any additional equipment or infrastructure [4]. This process, developed in the early 1990s [5,6], is based on the ability of alkali and alkali earth elements to store NO_x in the form of nitrites and nitrates [7] under lean-burn conditions. Subsequently, under a stoichiometric or rich-fuel environment, the stored NO_x is released and reduced with hydrocarbons, CO or H_2, to form N_2, H_2O, and CO_2 [5,8]. Thus, the NSR catalysts require an oxidation component, typically a noble metal (e.g., Pt), a storage component (commonly Ba or BaO), and a high-surface area support (e.g., γ-Al_2O_3). Potassium is another element that has shown potential as a storage component with a significant benefit at higher temperatures; the K-based nitrate is more stable than the typical Ba nitrate [9–11]. Previous studies [12,13] have demonstrated the good performance of K-based lean NO_x trap catalysts, even in the presence of CO_2 and H_2O in the feed. In addition, Toops et al. [14] recently carried out DRIFTS experiments to elucidate the key steps in the adsorption of NO_x on Pt–K/Al_2O_3 and illustrated the limiting regimes associated with NO_x adsorption: kinetic limitations at low temperatures and insufficient storage sites at high temperatures. Thus, the efficiency of the NSR catalysts depends strongly on several factors, including the rate and efficiency of each step (e.g., oxidation of NO into NO_2, trapping capacity, reduction of desorbed NO_x), the duration of the two sequences (trapping and reduction process), and the amount of storage component. The modification and optimization of some of these variables could hardly be carried out with a conventional powder catalyst, however.

The idea of using solid electrolyte cells for the electrochemical trapping and regeneration of NSR catalyst came from the phenomenon of electrochemical promotion, discovered and developed by the group of Vayenas [15,16]. This phenomenon is based on the control, by an applied potential, of an ion promoter concentration

* Corresponding author. Fax: +34 926295256.
E-mail address: joseluis.valverde@uclm.es (J.L. Valverde).

0021-9517/$ – see front matter
doi:10.1016/j.jcat.2008.07.008

at the surface of a working metal catalyst, which allows control of the strength of the chemical bonds between the metal and the adsorbates [17,18]. In addition, the use of an electrochemical catalyst, in which the ions electrochemically transferred from the support can effectively act as a storage component (e.g., potassium ions), would allow in situ control of the trapping and desorption of NO_x, as well as the storage component loading on the catalyst surface. Li and Vernoux [19] used a Pt–Ba/YSZ electrochemical catalyst for the NSR process and found that the variation in the open circuit potential in the cell was an effective indicator for the subsequent in situ NO_x storage reduction process. However, in that work, the use of an O^{2-} conductor as a solid electrolyte support did not allow electrochemical trapping of NO_x or regeneration of the catalyst surface. To the best of our knowledge, apart from a previous short communication by MacLeod et al. [20], the literature contains no studies of the direct electrochemical trapping and regeneration of NSR catalyst. MacLeod et al. [20] explored the possibility of trapping NO_x on sodium sites electrochemically generated on a Pt catalyst by using a Na–βAl_2O_3 wafer as the solid electrolyte. They did not investigate either the mechanism of the phenomenon or on the influence of the operation conditions in depth, however.

The present study was undertaken to investigate the electrochemically assisted NSR catalyst by a solid electrolyte cell. The tubular configuration of the electrochemical catalyst (Pt/K–βAl_2O_3) used could be important not only for fundamental studies of NO_x storage-reduction process, but also from a practical standpoint. Moreover, in this study the effect of the reaction temperature, the storage component supplied rate and loading, the presence of water in the feed, and the ability of the system to work without changes in the gas composition on the efficiency of the electrochemical catalyst to store and reduce NO_x was considered. In addition, temperature-programmed desorption experiments of NO_x (NO_x-TPD) and cyclic voltammetry measurements were carried out to investigate the chemisorption properties of the electrochemical catalyst at varying catalyst potentials.

2. Experimental

The tubular electrochemical catalyst consisted of a porous, continuous thin Pt film (geometric area of 45 cm^2) deposited inside a 18-mm-i.d., 40-mm-long, 1-mm-thick K–βAl_2O_3 tube (Ionotec). A gold counterelectrode was deposited on the outer side of the solid electrolyte tube to perform polarizations. Both electrodes were prepared using metal pastes and annealed at 800 °C for 12 h in air. The final Pt loading was 3.5 mg Pt/cm^2. Before the electrochemical trapping experiments, the catalyst was reduced in a stream of H_2 at 400 °C for 1 h. The surface mol (mol of active sites) of the catalyst-electrode film was characterized by the electrochemical technique developed by Ladas et al. [21] and found to be 9.7×10^{-5} mol Pt (3.8 m^2). The obtained Pt surface area of this tubular configuration was more than 200 times greater than that typically obtained in our previous single-pellet configurations [22,23], to achieve suitable values of NO_x storage/reduction activities.

The electrochemically assisted NO_x storage/reduction experiments were performed at atmospheric pressure in a tubular solid electrolyte cell reactor as described previously [24]. The tubular electrochemical catalyst was placed on a fritted quartz 21 mm in diameter. An inner quartz tube was connected to the Pt catalyst's working electrode to ensure electrical contact. All of the current collectors in the reactor were made from gold, which was catalytically inert in the process. The temperature of the catalyst was measured with a K-type thermocouple (Thermocoax) placed inside the inner quartz tube. The entire reactor was placed in a furnace (JH HEE.CC4) equipped with a heat control system (Conatec 4801). Constant voltages across the cell were imposed using a potentiostat–galvanostat (Voltalab 21; Radiometer Analytical). The reaction gases were Praxair-certified standards of 4% C_3H_6/He, 4% NO/He, O_2 (99.99% purity), and He (99.999% purity), which was used as the vector gas. The gas flow was controlled by a set of calibrated mass flowmeters (Brooks 5850 E and 5850 S), and water was introduced to the reacting stream by means of a saturator. The water content in the reaction mixture was controlled using the vapour pressure of H_2O at the temperature of the saturator (30 °C). The tubing downstream from the saturator was heated to 100 °C to prevent condensation. The dynamic storage/reduction experiments were performed using a series of periodic operations from lean burn conditions (1000 ppm of NO, 1000 ppm of C_3H_6, 5% of O_2, He balance) to rich conditions (1000 ppm of NO, 1000 ppm of C_3H_6, 0.5% of O_2, He balance) at different temperatures (250–370 °C). The overall gas flow rate during the lean and rich periods was kept constant at 15 $L\,h^{-1}$. The effect of water steam on the NSR yield was evaluated with the presence of 5% H_2O in the above reactants gas composition. During the lean-burn period, a negative potential between −0.5 V and −2 V was applied between the catalyst's working electrode and the counterelectrode to transfer K^+ ions from the electrolyte to the Pt catalyst and thereby create storage sites. During the regeneration period (rich conditions), a positive potential of 3 V was applied to release the NO_x to the gas phase and to regenerate the Pt surface. Reactant and product gases were analyzed with a micro gas chromatograph (Varian CP-4900) and a chemiluminescence analyzer (Teledyne 9110 EH). Before these analyses, the water was trapped by a condenser at −5 °C. To evaluate the activity of the electrochemical catalyst exclusively due to the storage reduction process, the conversion of NO_x to N_2 was calculated using the following equation:

$$NO_x \text{ conversion } (\%) = (NO_{x\,\text{storage}} - NO_{x\,\text{release}})/NO_{x\,\text{fed}} \times 100\ (\%), \quad (1)$$

where $NO_{x\,\text{storage}}$ denotes the amount of NO_x trapped in the lean period, $NO_{x\,\text{release}}$ denotes the amount of NO_x decomposed during the rich period and not reduced to N_2, and $NO_{x\,\text{fed}}$ is the total amount of NO_x fed to the reactor during the trapping and decomposition of the NO_x.

NO_x-TPD experiments were carried out in the tubular cell reactor as mentioned earlier. The working electrode was first reduced under H_2 at 400 °C for 1 h and then purged under He for 30 min and cooled to 300 °C. The lean atmosphere (1000 ppm of NO, 1000 ppm of C_3H_6, 5% of O_2, He balance) was then introduced in the reactor at 300 °C with a continuous flow of 15 $L\,h^{-1}$, under application of a constant potential between 3 and −2 V for 30 min. Then the sample was cooled to 50 °C under the same conditions and purged with pure He with a constant flow of 9 $L\,h^{-1}$ for 30 min under open-circuit conditions. Finally, the sample temperature was increased at a rate of 5 °C min^{-1} up to 400 °C, under application of a constant applied potential between 3 and 0.5 V and He atmosphere. During the TPD experiments, NO_x concentration was continuously monitored with the chemiluminescence analyzer.

Cyclic voltammetry measurements in conjunction with NO_x analysis were performed with the potentiostat–galvanostat under lean reaction conditions (1000 ppm of NO, 1000 ppm of C_3H_6, 5% of O_2, He balance). Cyclic voltammograms were recorded at the same temperature as for the adsorption experiments (300 °C), between 3 and −2 V at a constant sweep rate of 5 $mV\,s^{-1}$.

3. Results and discussion

3.1. NSR transient operation under lean/rich conditions

The possibility of electrochemical trapping and regeneration of the Pt catalyst for the effective abatement of NO_x was first

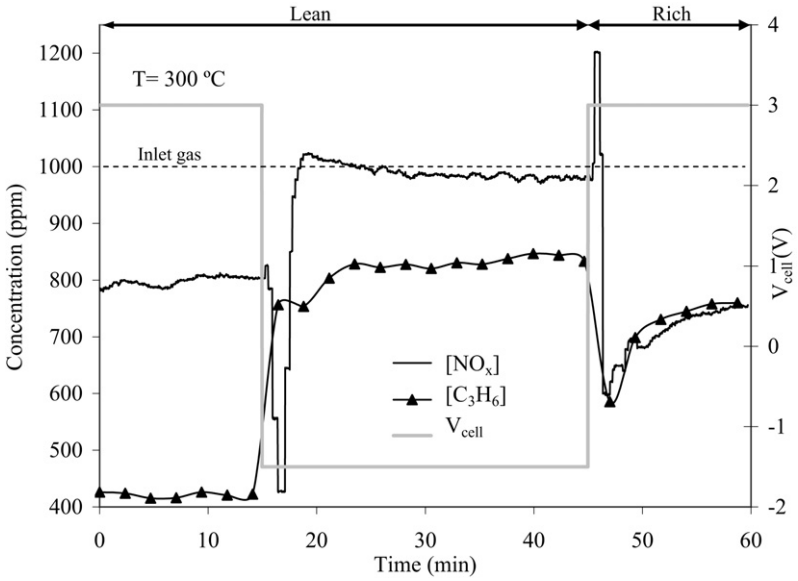

Fig. 1. NO_x and C_3H_6 outlet concentration profiles vs. time during NO_x storage/reduction experiments at 300 °C. Lean phase ($NO/C_3H_6/O_2$: 1000 ppm/1000 ppm/5% O_2), $V_{cell} = -1.5$ V, 30 min of duration. Rich phase ($NO/C_3H_6/O_2$: 1000 ppm/1000 ppm/0.5% O_2), $V_{cell} = 3$ V, 15 min of duration.

investigated at 300 °C. Fig. 1 shows the outlet NO_x and C_3H_6 concentration profiles versus time during the transient from lean ($NO/C_3H_6/O_2$: 1000 ppm/1000 ppm/5%) to rich conditions ($NO/C_3H_6/O_2$: 1000 ppm/1000 ppm/0.5%) under different applied catalyst potentials (V_{cell}). At $t = 0$ min, the gas was switched to the lean composition, and a catalyst potential of 3 V was applied to keep the Pt surface free of potassium ions and to define a reproducible state of the catalyst. Under these conditions, the outlet NO_x concentration was approximately 800 ppm, due to the SCR activity of the Pt film free of alkali ions [24,25], whereas the C_3H_6 concentration was much lower (400 ppm). This was attributed to the consumption of hydrocarbon not only in the SCR process, but also to its direct combustion with O_2. Subsequent application at $t = 15$ min of a constant potential of −1.5 V under lean atmosphere resulted in a significant decrease in the NO_x concentration and a significant increase in the C_3H_6 concentration. Under these conditions, potassium ions were electrochemically transferred from the electrolyte to the Pt surface, leading to a modification of the binding strength of chemisorbed reactants [17, 22–26]. At first glance, this suggests that the presence of alkali ions increased the SCR activity of the Pt catalyst; however, previous studies of electrochemical promotion using cationic conductors [24,25] have shown that under lean burn conditions and high reaction temperatures (300 °C), when most of the C_3H_6 was burned, the application of very negative polarizations (i.e., −1.5 V) led to a significant decrease in the SCR activity. Under these conditions, a decrease in the catalyst potential led to a pronounced increase of the oxygen coverage on the catalyst and inhibition of C_3H_6 adsorption [27], which caused the observed decrease in the C_3H_6 reaction rate. This assumption can be further confirmed, as it will be shown in the next figure, by the observed increase in the NO oxidation activity under application of the negative polarization, due to an increase in the coverage of O adsorbed atoms (O_{ads}) at the expense of C_3H_6. Therefore, the origin of the NO_x concentration decrease seen in Fig. 1 can be attributed to the ability of the electrochemical catalyst to temporarily store NO_x in the form of potassium nitrates [12–14]. This phenomenon (electrochemical trapping of NO_x) can be verified by the decomposition of part of the stored nitrates during the positive polarization under rich conditions (electrochemical regeneration). Thus, during the electrochemical trapping of NO_x in the lean phase, the NO_x concentration decreased to a minimum of around 450 ppm at $t = 17$ min. After this time, NO_x concentration began to increase until it matched the inlet value, indicating that the available trapping sites were saturated, and thus the catalyst trapping ability under these conditions was finished. Therefore, the high amount of NO_x trapped during the negative polarization (10.2 μmol) likely led to excessive formation of potassium nitrate, which blocked most of the Pt active sites, leading to negligible SCR activity [27]. Nevertheless, the total amount of NO_x trapped was much lower than the total number of Pt active sites measured by the galvanostatic transient (97 μmol). It can be attributed to the high molar volume of nitrates, which can cover or block a high number of Pt sites [28]. In addition, under these conditions, propene conversion decreased due to the low quantity of available free Pt active sites. At $t = 45$ min, the inlet gas was switched to the rich mixture, and a catalyst potential of 3 V was applied for other 15 min. Under such conditions, a rapid increase in the outlet NO_x concentration was observed in the first seconds, possibly because the catalyst's ability to store NO_x decreased at lower O_2 concentrations [29], followed by the release of stored NO_x from the catalyst under positive polarization. The NO_x concentration decreased quickly during the rich phase, however. Under positive polarization, potassium ions returned to the solid electrolyte [22,23], and part of the previously stored NO_x was reduced by C_3H_6 to N_2, regenerating the Pt catalyst surface. The integral amount of NO_x released was 0.95 μmol, and thus 90% of stored NO_x was reduced to N_2. In agreement with previous studies of Pt-based NO_x trapping catalyst [3], no trace of N_2O was observed during the reduction of stored nitrates. In addition, during the rich period, under application of 3 V, NO_x and C_3H_6 concentrations achieved a minimum value. We suggest that during the positive polarization (removal of potassium nitrates from the catalyst), an optimum potassium coverage was obtained for the SCR and hydrocarbon combustion process. Thus, it has been reported [23] that under rich conditions, low alkali coverage enhances both reactions. Therefore, in addition to the electrochemical trapping and regeneration phenomena, a positive NEMCA effect occurred for the SCR process during the regeneration period of the catalyst surface. This produced an additional increase in the yield of the system to remove NO_x that was not considered by Eq. (1) to study the NSR process exclusively. At $t = 60$ min, a steady-state NO_x concentration around 750 ppm was achieved, indicating significantly greater SCR activity of the clean Pt catalyst (3 V) under rich atmosphere (0.5% O_2)

compared with the previous lean atmosphere (5% O_2). However, the C_3H_6 concentration achieved a higher value compared with that under lean conditions, due to the greater tendency of the hydrocarbon to react with O_2 [24]. In short, Fig. 1 clearly shows the possibility of using a solid electrolyte cell to electrochemically trap NO_x and regenerate an NSR catalyst to reduce NO_x to N_2 with a reasonable efficiency. The in situ electrochemical generation of potassium trapping sites instead of sodium ones, as shown in a previous study [20], probably led to higher efficiencies of the NSR process, due to the greater stability of potassium nitrates compared with sodium ones [30].

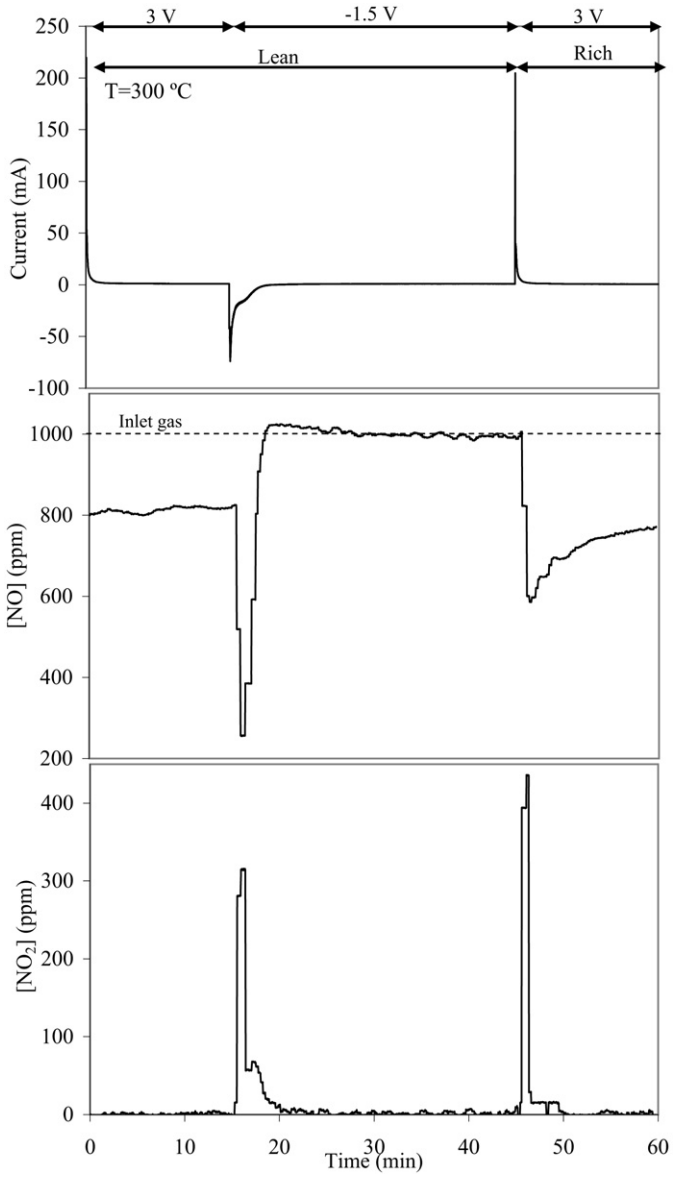

Fig. 2. Current and NO/NO_2 outlet concentration profiles vs. time during NO_x storage/reduction experiments at 300 °C. Lean phase ($NO/C_3H_6/O_2$: 1000 ppm/1000 ppm/5% O_2), $V_{cell} = -1.5$ V, 30 min of duration. Rich phase ($NO/C_3H_6/O_2$: 1000 ppm/1000 ppm/0.5% O_2), $V_{cell} = 3$ V, 15 min of duration.

To further explore the mechanisms of electrochemical trapping and catalytic reduction of NO_x, the current as well as the [NO] and [NO_2] concentrations versus time was studied for the previous experiment (Fig. 2). Under lean conditions, the application of a negative polarization of −1.5 V caused the migration of potassium ions from the solid electrolyte to the catalyst, with the concomitant formation of a compound (negative current) between potassium ions and the different adsorbed species on the catalyst surface [22,24]. However, under rich conditions, during the positive polarization, potassium ions returned to the solid electrolyte, leading to decomposition of the previously formed potassium compound (positive current). According to previous studies of the NSR catalyst [31,32], the steps involved in these two parts of the cycle can be summarized as follows:

1. NO oxidation to NO_2.
2. NO_2 and NO adsorption in the form of nitrites or nitrates.
3. Reductant evolution when the exhaust is switched to the rich condition.
4. Nitrate decomposition resulting in NO_x release or migration to reduction sites.
5. NO_x reduction to N_2.

Fig. 3 integrates these steps in the transients of Figs. 1 and 2. From Fig. 2, it can be observed that under lean conditions, a decrease in the catalyst potential at $t = 15$ min led to an increase in the NO_2 (3.4 μmol) concentration at the expense of NO (13.6 μmol). This indicates that the presence of potassium ions promotes NO oxidation (step 1), as was observed in a previous study in which potassium was chemically added on a Pt catalyst [33]. The promotional effect of potassium was attributed to an increase in the O_2 adsorption rate, which has been identified as the rate-determining step for NO oxidation [34]. Thus, the increase in the NO oxidation reaction rate induced by the potassium ions initiated the NO_x storage process shown in Fig. 1. It also indicated (as already reported [19,35]), that the initial step of NO oxidation to NO_2 is the rate-limiting step in the NSR process. This promotional singularity of potassium involves an additional advantage of potassium-based NO_x trapping, because a catalyst containing platinum and barium has lower NO oxidation activity than the catalyst containing only Pt [36]. Simultaneously, potassium ions electrochemically pumped to the Pt catalyst active sites act as storage components and trap part of the NO and NO_2 in the form of nitrites and nitrates (step 2). According to previous studies [14], at temperatures above 200 °C, potassium nitrites are quickly oxidized to nitrates, which are likely the primary storage phase. Therefore, the negative current curves during the negative polarization shown in Fig. 2 indicate the rate of NO_x trapping. Thus, at $t = 19$ min, when the storage process was completed (Fig. 1), the NO concentration

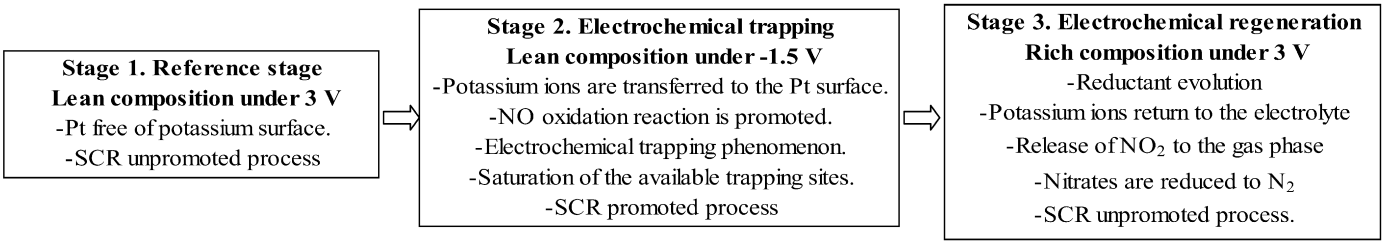

Fig. 3. Schematic representation of the main stages involved during an electrochemical assisted NO_x storage/reduction experiment.

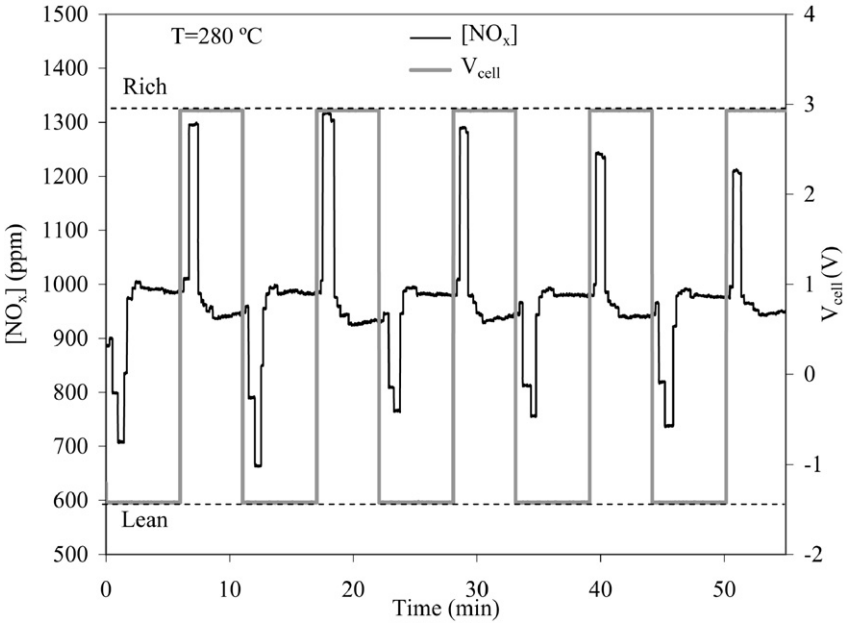

Fig. 4. NO_x outlet concentration profile vs. time during five consecutive NO_x storage/reduction cycles at 280 °C. Lean phase ($NO/C_3H_6/O_2$: 1000 ppm/1000 ppm/5% O_2), 6 min of duration, $V_{cell} = -1.5$ V. Rich phase ($NO/C_3H_6/O_2$: 1000 ppm/1000 ppm/0.5% O_2), 5 min of duration, $V_{cell} = 3$ V.

was 1000 ppm (equal to the inlet concentration), and the production of NO_2 and the current values were negligible. Under these conditions, the Pt active sites were totally covered by the stored nitrates, and the NO_x trapping, NO oxidation, and SCR processes were negligible. During the rich atmosphere step, the application of 3 V desorbed part of the stored nitrates as NO_2 (2.95 μmol), and potassium ions returned to the catalyst, as evidenced by the positive current leading to steps 3, 4, and 5. When the catalyst surface was completely regenerated, the current decreased to zero, and some of the inlet NO was reduced by C_3H_6 (SCR) on potassium-free Pt catalyst. Note that one of the most important issues illustrated in Fig. 2 is that the variation of the current versus time curves followed exactly the same trend as the NSR process. It allowed us to monitor the time at which the catalyst was totally saturated in the lean period and also the time at which it was totally regenerated in the rich period. In a previous study, Li and Vernoux [19] used a similar configuration of Pt–Ba/YSZ, where the measurement of the catalyst potential allowed them to follow the NSR process on the chemically added Ba sites. An additional advantage of the present configuration, in which the trapping sites are in situ electrochemically supplied or removed, versus that of Li and Vernoux [19] is that it allows the trapping and regeneration processes to be not only followed, but also controlled. However, in either of the two configurations, the system's ability to optimize the duration of the lean and rich sequences, measuring just the potential or the current, implies an important advance in the technological application of this NSR process that is not possible with a convectional catalyst, for which an NO_x detector is required. Thus, according to the results of Figs. 1 and 2, the durations of the lean and rich periods were decreased in successive experiments to improve the system's performance.

To evaluate the reproducibility of the electrochemical trapping and regeneration experiments, five consecutive cycles from lean ($NO/C_3H_6/O_2$: 1000 ppm/1000 ppm/5%, $V_{cell} = -1.5$ V, 6 min of duration) to rich conditions ($NO/C_3H_6/O_2$: 1000 ppm/1000 ppm/0.5%, $V_{cell} = 3$ V, 5 min of duration) were carried out. Fig. 4 displays the NO_x concentration profile obtained for the consecutive cycles at 280 °C. Table 1 summarizes the amounts of NO_x trapped, released, and reduced to N_2 for each cycle. Reasonable reproducibility between the different cycles can be seen, which can be further confirmed by looking at numbers of Table 1. For instance, the amount of electrochemically trapped NO_x seemed to achieve a steady value, implying that the applied catalyst potential of 3 V during the 5-min rich period was sufficient to remove all of the potassium nitrates stored in the lean phase, and thus to completely regenerate the catalyst surface. The Au counterelectrode behaved reversibly over many cycles (not shown here), because in any given experiment, the alkali depletion of the bulk electrolyte was negligible and was restored when the current was reversed. Thus, integration of the current/time curves obtained during the lean-rich cycles, as shown in Fig. 2, indicates that equal amounts of potassium were pumped to and from the electrolyte during the trapping and regeneration periods. On the other hand, the low percentages of trapped NO_x, shown in Table 1, can be attributed to bypass of the reactive mixture to the Pt catalyst due to the geometry of the cell. Elimination of the bypass (about 30%, estimated from the combustion of the hydrocarbon at high temperature) to improve the efficiency of NSR performance will be considered in future studies. Fig. 4 and Table 1 also show that continuous operation of the electrochemical catalyst between the lean and rich periods seems to increase the catalytic performance of the system slightly, because more NO_x was reduced to N_2 in the last two cycles. This can be attributed to stabilization of the Pt catalyst morphology and the total removal of the Pt precursor under working conditions.

Table 1
NO_x trapped, released, and reduced to N_2, and percentage trapped during five consecutive NO_x storage/reduction cycles at 280 °C. Lean phase ($NO/C_3H_6/O_2$: 1000 ppm/1000 ppm/5% O_2), 6 min of duration, $V_{cell} = -1.5$ V. Rich phase ($NO/C_3H_6/O_2$: 1000 ppm/1000 ppm/0.5% O_2), 5 min of duration, $V_{cell} = 3$ V

Cycle	NO_x trapped (μmol)	Percentage trapped (%)	NO_x released (μmol)	NO_x reduced to N_2 (μmol)
1	3.83	6.25	2.27	1.56
2	3.98	6.50	2.89	1.09
3	3.30	5.38	1.91	1.38
4	3.49	5.69	1.76	1.73
5	3.98	6.49	1.33	2.65

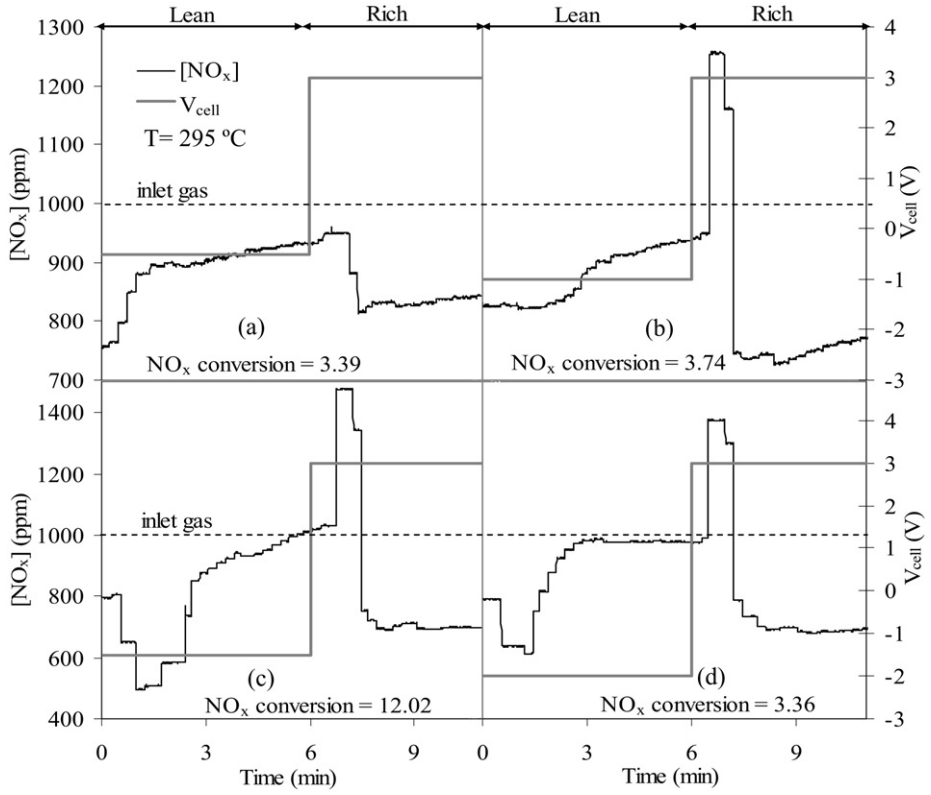

Fig. 5. NO_x outlet concentrations profile vs. time during NO_x storage/reduction experiments at 295 °C at different applied catalyst potentials for the lean phase: (a) −0.5 V, (b) −1 V, (c) −1.5 V and (d) −2 V. Lean phase ($NO/C_3H_6/O_2$: 1000 ppm/1000 ppm/5% O_2), 6 min of duration. Rich phase ($NO/C_3H_6/O_2$: 1000 ppm/1000 ppm/0.5% O_2), 5 min of duration, $V_{cell} = 3$ V.

3.2. Effect of potential on storage capacity

It is evident that the use of an electrochemically trapped/regenerated NSR catalyst opens up a new range of variables that can be modified in situ to improve the system's performance. For instance, Fig. 5 shows the NO_x concentration profile versus time for NSR experiments carried out under different negative polarizations in the lean phase: (a) −0.5 V, (b) −1 V, (c) −1.5 V, and (d) −2 V. Fig. 5 also depicts the NO_x conversion to N_2 achieved in each cycle attributed exclusively to the NSR process and measured by Eq. (1). Fig. 5 clearly shows that the value of the applied negative polarization strongly influences the NO_x concentration profile during the lean and rich periods. Thus, the greatest efficiency for NO_x removal was observed for cycle (c), in which a negative polarization of −1.5 V was applied during the lean phase. The NO_x concentration in the lean phase decreased to 500 ppm, and an optimum NO_x conversion to N_2 of 12% was obtained. Fig. 6 shows the influence of the negative polarization applied in each cycle of the previous experiments on both the total amount of NO_x stored and on the total amount of K^+ ions electrochemically transferred to the catalyst surface. This latter parameter can be measured according to Faraday's law [Eq. (2)] by integration during the lean phase ($t = 6$ min) of the current versus time curves obtained for each cycle (inset of Fig. 6),

$$\text{mol of potassium transferred} = \int_0^t \frac{I}{F}\,\mathrm{d}t, \tag{2}$$

where I is the current and F is the Faraday constant. Fig. 6 shows that the amount of NO_x storage during the lean period increased with the decrease in catalyst potential from −0.5 V to −1.5 V. Under these conditions, the increasing number of potassium ions transferred to the catalyst surface likely increased the promotional effect of NO_2 formation [33], which also reacted with a greater number of potassium-trapping sites located on the catalyst surface, leading to the adsorption of more potassium nitrates [14]. Thus, for cycles (a) and (b), the NSR process was limited by the number of potassium ions transferred to the catalyst, which prevented its saturation. Consequently, the NO_x concentration at the end of the lean phase did not achieve the inlet value (Fig. 5). However, for cycle (c), the high amount of stored NO_x resulting from the greater quantity of potassium ions transferred to the catalyst led to a total blockage of Pt active sites and negligible final SCR activity during the lean phase. On the other hand, a further decrease in the applied negative polarization to −2 V for the lean phase did not correspond to an increase in the amount of NO_x stored. The application of a negative polarization of −2 V led to very negative currents (Fig. 6, inset), which likely led to some poisoning of the Pt sites for the NO oxidation reaction. In this case, the high rate of electrochemically transferred potassium ions likely led to excessive adsorption of O_2. Under negative polarization, the adsorption of electron acceptor species, such as O_2 and NO, is enhanced [17, 22–27]. But O_2 is known to be a stronger electron acceptor than NO [22–27]; therefore, when the catalyst potential decreased to very low values, the excessive coverage of O_{ads} could limit the adsorption of NO and thus the formation of NO_2. Therefore, under these conditions, the high coverage of O adsorbed on the catalyst instead of NO and NO_2 likely led to the preferential formation of potassium oxides and peroxides instead of potassium nitrates, decreasing the ability of the electrochemical catalyst to store NO_x. The formation of such oxides and peroxides has been identified as an initial step in the activation of potassium for trapping NO_x [14]. Subsequently, the reaction of such potassium oxides and peroxides with adsorbed NO and NO_2 leads to the formation of stored potassium nitrates [14]. However, the excess of O_{ads} on the catalyst surface induced by the high number of potassium ions supplied

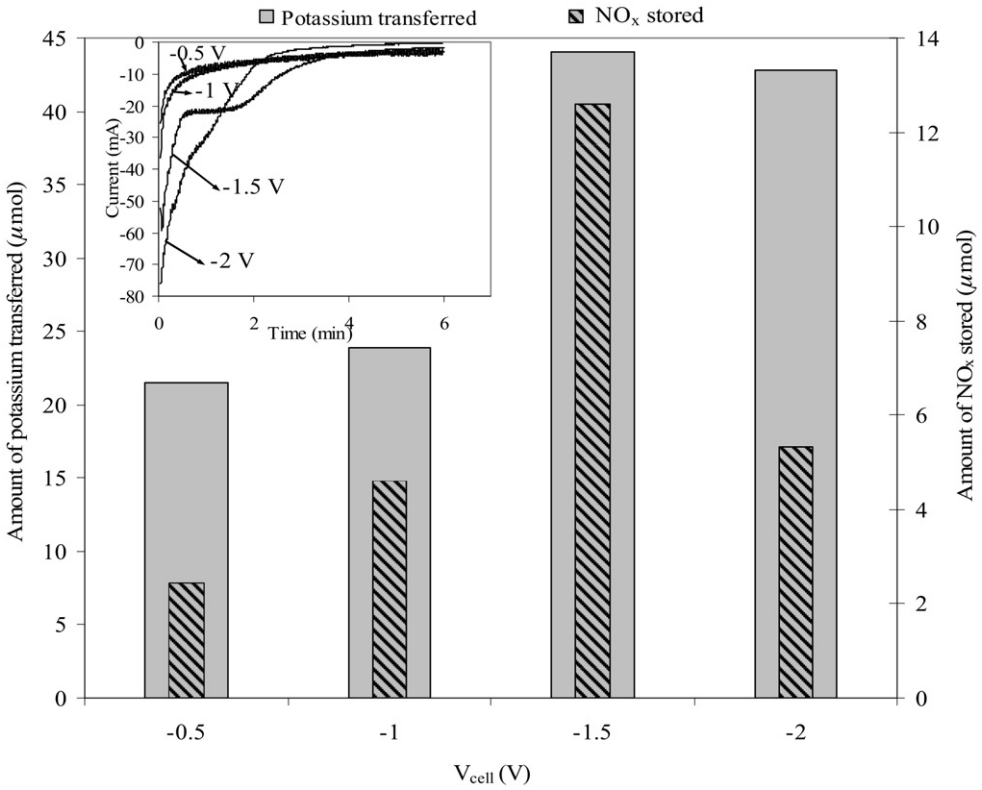

Fig. 6. Influence of the applied catalyst potential during the lean phase on the amount of potassium electrochemically transferred to the catalyst and on the amount of NO_x stored. Inset: Current vs. time curves during the lean phase at varying catalyst potentials. Lean phase ($NO/C_3H_6/O_2$: 1000 ppm/1000 ppm/5% O_2), 6 min of duration. Rich phase ($NO/C_3H_6/O_2$: 1000 ppm/1000 ppm/0.5% O_2), 5 min of duration, $V_{cell} = 3$ V.

under −2 V likely decreased the adsorption of NO and formation of NO_2, decreasing the amount of stored nitrates compared with a potential of −1.5 V. Thus, under these conditions (−2 V), most of the potassium ions electrochemically pumped to the catalyst remained as potassium oxides/peroxides, leading to the greatest difference between the amount of NO_x stored and the amount of potassium ions transferred (Fig. 6). The presence of such potassium oxides and peroxides phases under similar reaction conditions on a Pt/K–βAl_2O_3 electrochemical catalyst was previously reported by our group [22]. The nature of such potassium oxide and peroxide phases have been discussed in detail elsewhere [12–14,37,38], with the leading candidates being K_2O. As noted earlier, the double role of potassium as NO oxidation-promoting and storage sites implies that not only its total amount, but also the transfer rate to the Pt catalyst, influence the yield of the solid electrolyte cell to electrochemically trapped NO_x. Thus, a balance between these two variables should be considered to improve the efficiency of the process through the application of moderately negative potentials (e.g., −1.5 V).

3.3. Effect of temperature on storage capacity

We also investigated the effect of the reaction temperature on the efficiency of the electrochemical catalyst in the NSR process. Fig. 7 shows the NO_x concentration profile during the first 3 min of the lean phase (total duration, 6 min), under application of a catalyst polarization of −1.5 V at different reaction temperatures. First, it is interesting to note the ability of the solid electrolyte cell to electrochemically trap NO_x, even at low reaction temperatures (250 °C). This property can be attributed to the ability of potassium ions to promote the NO oxidation reaction above 200 °C [33]. As expected, the shape of the curves changed as a function of the reaction temperature. Fig. 8 summarizes the effect of the reaction temperature on the amount of NO_x trapped, the amount of potassium transferred during the lean phase, and the conversion of NO_x to N_2 obtained for the overall lean-rich cycle, measured by Eq. (1). It can be seen that the amount of NO_x trapped during the lean phase increased with an increase in reaction temperature from 250 °C to 350 °C; however, a further increase in the reaction temperature up to 370 °C did not correspond to an increase in the amount of NO_x stored. This observation is in good qualitative agreement with previous studies of an NSR catalyst based

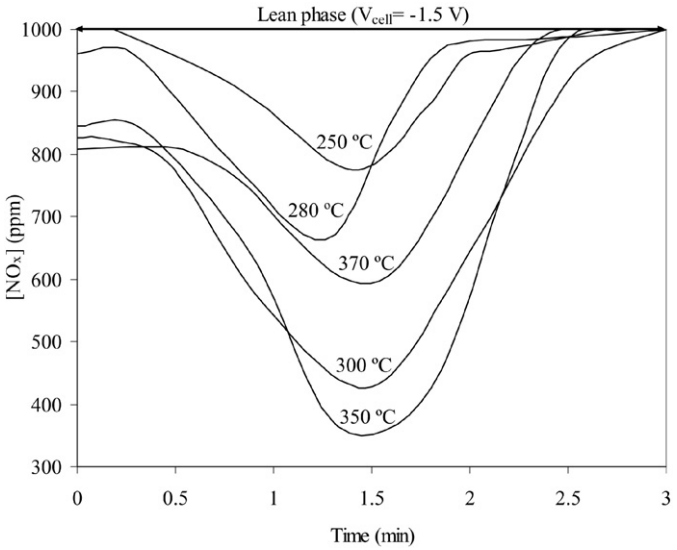

Fig. 7. NO_x outlet concentration profiles vs. time for the first 3 min of the lean phase during NO_x storage process at different reaction temperatures. Lean phase ($NO/C_3H_6/O_2$: 1000 ppm/1000 ppm/5% O_2), 6 min of duration, $V_{cell} = -1.5$ V.

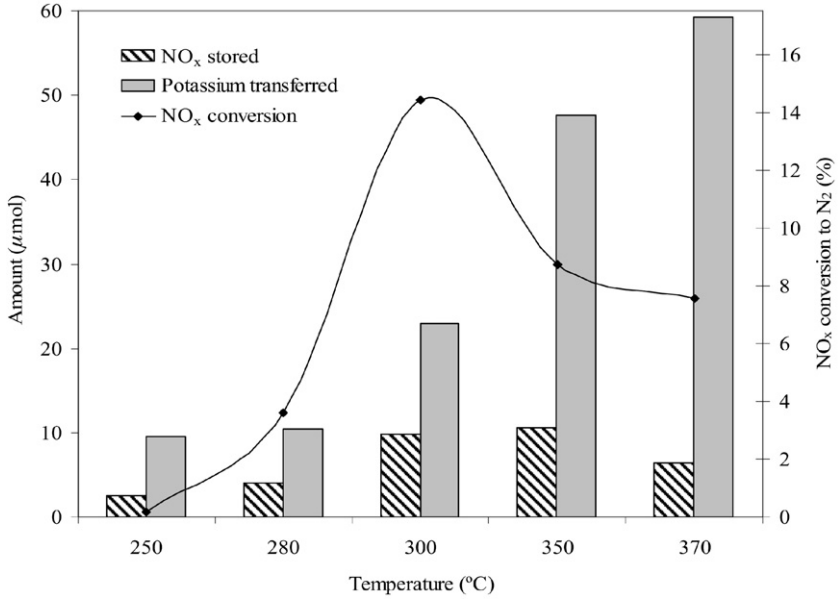

Fig. 8. Influence of the reaction temperature on the amount of NO_x stored, potassium transferred and on the NO_x conversion to N_2 during NO_x storage/reduction experiments. Lean phase ($NO/C_3H_6/O_2$: 1000 ppm/1000 ppm/5% O_2), 6 min of duration, $V_{cell} = -1.5$ V. Rich phase ($NO/C_3H_6/O_2$: 1000 ppm/1000 ppm/0.5% O_2), 5 min of duration, $V_{cell} = 3$ V.

on Ba [32]. As the reaction temperature increased, the NO oxidation rate improved [32,33]. This improvement was even greater for the Pt/K–βAl_2O_3 electrochemical catalyst, because of an increase of the ionic conductivity of the electrolyte. Thus, the amount of potassium ions electrochemically transferred to the catalyst for the same potential increased with the reaction temperature, causing an additional increase in the promotional effect of NO oxidation and the number of available storage sites. On the other hand, the diminished trapping performance observed at higher temperatures was due to a decrease in the nitrates' stability [32,39] which also increased the amount of NO_x released during the rich period. This caused the appearance of a maximum NO_x conversion at a certain temperature (Fig. 8), as observed in previous studies [35]. Note that the possibility of controlling the decomposition rate of the stored nitrates by applying positive potentials during the rich phase could lead to a significant improvement in the conversion. Thus, a decrease in the value of the applied catalyst potential during the regeneration phase likely led to increased nitrate stability (as we found based on NO_x-TPD measurements), and also very likely to improved efficiency of the catalyst at high reaction temperatures. This property is an important advantage of the electrochemically assisted NSR catalyst, allowing in situ modification of the adsorption/desorption rates of the stored nitrates.

3.4. Effect of water steam on storage capacity

To evaluate the performance of the electrochemical catalyst under real working conditions, we also considered the presence of water steam (5%). Fig. 9 shows the NO_x concentration profiles at two different reaction temperatures during the transient from lean ($NO/C_3H_6/O_2/H_2O$: 1000 ppm/1000 ppm/5%/5%) to rich conditions ($NO/C_3H_6/O_2/H_2O$: 1000 ppm/1000 ppm/0.5%/5%), under applied catalyst potentials of −2 V and 3 V, respectively. The durations of the lean and rich phases were reduced to 3.5 min each. The inset in Fig. 9 shows the NO_x conversion to N_2 observed at each reaction temperature. First, we note that the more negative potential applied under the presence of water steam (−2 V) in contrast with the previous experiments was due to the very low storage capacity demonstrated by the electrochemical catalyst under application of −1.5 V. Under these conditions, the system clearly was able

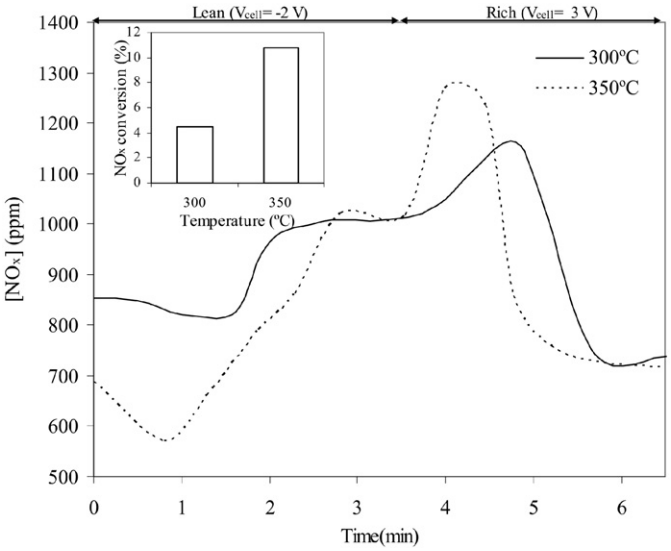

Fig. 9. NO_x outlet concentration profile vs. time under different applied catalyst potential during NO_x storage/reduction experiments under wet reaction conditions at different temperatures. Inset: Influence of the reaction temperature on the overall NO_x conversion to N_2. Lean phase ($NO/C_3H_6/O_2/H_2O$: 1000 ppm/1000 ppm/5%/5%), 3 min of duration, $V_{cell} = -1.5$ V. Rich phase ($NO/C_3H_6/O_2/H_2O$: 1000 ppm/1000 ppm/0.5%/5%), 3 min of duration, $V_{cell} = 3$ V.

to electrochemically trap NO_x under the presence of water in the feed, with a growing increase in the efficiency with increasing reaction temperature from 300 to 350 °C. But despite optimization of the duration time for the lean-rich periods, the NO_x conversion achieved by the electrochemical catalyst was decreased compared to the results obtained at dry conditions (Fig. 8). A similar decrease in the efficiency of NSR catalysts due to the presence of water steam in the feed has been described previously [40,41]. Lindholm et al. [40] attributed the inhibiting effect of water on Pt–Ba/Al_2O_3 to the formation of $Ba(OH)_2$, which has less storage capacity than BaO. Epling et al. [41] added that the presence of water reduces the number of active sites available for NO_x adsorption. These two explanations could be applied to elucidate the observed inhibiting effect of water steam in the performance of the electrochemical

catalyst. This inhibiting effect of water also has been observed on both Pt/Al_2O_3 and $Pt–K/Al_2O_3$ [33] for the NO oxidation reaction, the rate-limiting step for the NO_x storage process [19,35]; however, it was found [33] that the presence of water decreased the NO conversion on Pt/Al_2O_3 by a factor of 3, but decreased it on $Pt–K/Al_2O_3$ by a factor of 1.4. Our group recently observed a similar decrease in the inhibiting effect of water for the SCR of N_2O, due to electrochemical pumping of potassium ions to the Pt catalyst [23]. This decreased inhibiting effect has been attributed to decreased adsorption of water (electron-donor molecule) induced by the presence of electropositive potassium ions on the catalyst surface. Thus, we can assume that the additional role of potassium as an electropositive promoter in the NO oxidation reaction under wet conditions could decrease the inhibiting effect of water in the overall NSR process, improving the efficiency of $Pt/K–\beta Al_2O_3$ compared with other catalyst systems. Note that the resistance to water is an important factor in the development of any catalyst with the potential for NO_x removal. In this sense, $K–\beta Al_2O_3$ is significantly more stable than $Na–\beta Al_2O_3$ in the presence of water vapour [20]; for example, it survives long periods at 900 K and 15% humidity, much more severe conditions than those used here.

3.5. NSR operation under fixed lean conditions

We also investigated the possibility of electrochemical trapping and regeneration of solid electrolyte cell under a fixed lean gas composition. Fig. 10 depicts the NO_x concentration profile versus time under application of −1.5 V for 6 min during the electrochemical trapping step and also under application of 3 V for 5 min during the electrochemical regeneration, for a constant lean composition ($NO/C_3H_6/O_2$: 1000 ppm/1000 ppm/5%) at 320 °C. As can be seen from the two cycles depicted in Fig. 10, the solid electrolyte cell could electrochemically trap NO_x and be regenerated under a constant lean atmosphere with a reproducible behaviour. Under these interesting working conditions, the positive applied potential of 3 V was sufficient to completely regenerate the catalyst surface for a new storage cycle. Some release of NO_x also could be observed at the end of the lean phase, likely due to decomposition of part of the stored nitrates at this temperature ($T = 320$ °C) [32,39]. However, Fig. 10 shows an overall decrease in the amount of NO_x released in the entire process. The presence of an excess of O_2 during the regeneration phase likely stabilized the stored nitrates, decreasing NO_x release [42] and improving the system's efficiency. Thus, the driving force induced by the positive polarization was sufficient to decompose all of the stored NO_x, leading to reduction to N_2 and regenerating the catalyst surface for a new cycle. With a conventional NO_x trapping catalyst, regeneration usually is done by either injecting raw fuel upstream of the NSR catalyst or switching the gas mixture in the engine to an excess of reductant (fuel) relative to O_2 [43]. But the possibility of regenerating the catalyst surface by imposing a catalyst potential implies an important technological improvement and a relevant simplification of the NSR process, because it would avoid the periodic changes in the gas-phase composition, which is not always an easy task.

3.6. NO_x-TPD and cyclic voltammetry measurements

NO_x-TPD experiments were first carried out after NO_x adsorption at 300 °C on the catalyst surface at 3 and −2 V under lean conditions (1000 ppm of NO, 1000 ppm of C_3H_6, 5% of O_2, He balance). Fig. 11 shows the results of the NO_x-TPD experiments under application of 3 V. No desorption peaks of NO_x were observed when the adsorption was carried out over a potassium-free Pt surface; however, two desorption peaks were observed when

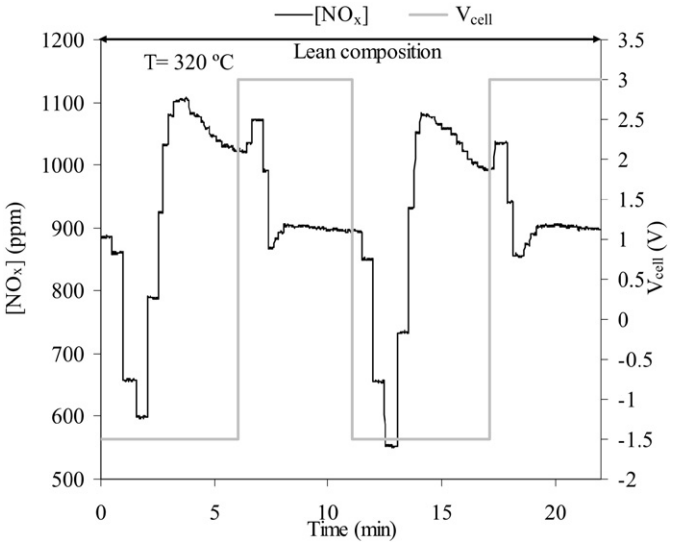

Fig. 10. NO_x outlet concentration profile vs. time during NO_x storage/reduction experiments under a fixed lean reaction composition ($NO/C_3H_6/O_2$: 1000 ppm/1000 ppm/5%) at 320 °C. Storage phase: −1.5 V, 6 min of duration. Regeneration phase: 3 V, 5 min of duration.

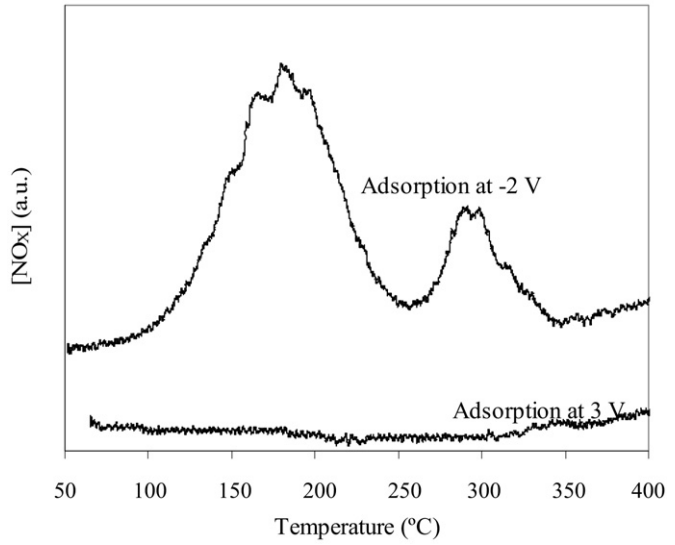

Fig. 11. NO_x desorption profile vs. temperature under application of 3 V. Adsorption conditions: $NO/C_3H_6/O_2$: 1000 ppm/1000 ppm/5%, 30 min of duration, $V_{cell} = 3$ and −2 V.

the adsorption was carried out on the potassium-modified Pt surface (i.e., under application of −2 V). The figure shows that all of the desorbed NO_x came from the stored nitrates during the adsorption step under negative polarization, because no desorption peaks of NO_x adsorbed on the clean Pt film are seen. These results clearly demonstrate that NO_x was weakly adsorbed on the large Pt particles obtained using Pt paste [19]. But the two desorption peaks obtained after adsorption at −2 V indicate the presence of two different nitrate species on the NO_x-saturated Pt–K surface. Similar NO_x-TPD results, with two desorption temperature peaks, have been found after NO_x was adsorbed on BaO/γ-Al_2O_3 samples [44,45]. Those studies showed that two types of nitrates could be formed on the catalyst: surface nitrates, which decompose first, and bulk alkaline nitrates, which decompose at higher temperatures. We propose that, similar to BaO/γ-Al_2O_3, the lower-temperature desorption peak at around 180 °C is related to desorption of surface nitrates, whereas the higher-temperature de-

sorption peak at 300 °C is due to decomposition of bulk potassium nitrates. Compared with a previous study [45], here the desorption peaks were observed at much lower temperatures. This can be attributed to the application of a catalyst potential of 3 V during the TPD, which strongly favoured decomposition of the stored nitrates. Fig. 12 shows the results of the NO_x-TPD carried out at different catalyst potentials. In this case, the adsorption step was carried out at 300 °C under lean conditions (1000 ppm of NO, 1000 ppm of C_3H_6, 5% of O_2, He balance) under application of −2 V, with different positive potentials (0.5, 2, and 3 V) applied during TPD. The results clearly show that the maximum desorption temperature of the stored nitrates can be modified by varying the applied catalyst potential. Thus, as the catalyst potential was increased from 0.5 V to 3 V, the decomposition of both stored nitrates (surface and bulk) were favoured. For the TPD carried out at 0.5 V, desorption of the surface nitrates (lower temperature desorption peak) did not begin until 380 °C, and decomposition of the bulk nitrate (higher-temperature peak) did not occur in the temperature range investigated. In this case, the maximum desorption temperature peaks of the stored nitrates approached those reported previously for BaO/γ-Al_2O_3 samples [44,45]; however, the application of higher potentials strongly decreased the maximum desorption temperature peaks. Under application of 2 V and (3 V), desorption of the surface nitrate occurred at 195 °C and (185 °C), whereas decomposition of the bulk nitrate occurred at around 390 °C and (295 °C). Thus it is clear, as mentioned earlier, that a solid electrolyte cell allows control of the thermal stability of the electrochemically stored nitrates and thus modification of the chemisorption properties of the catalyst, in good agreement with the current theory of electrochemical promotion [17,18]. In addition, the TPD carried out under application of 3 V demonstrated release of all of the stored nitrates at around 300 °C (see Fig. 10). This suggests the possibility of electrochemically regenerating the catalyst surface at this temperature, and thus the system's ability to work under a fixed lean composition. In addition, the NO_x-TPD measurements demonstrate that potassium nitrates were preferentially adsorbed on the catalyst as surface species, although an important portion also existed as bulk alkali compounds.

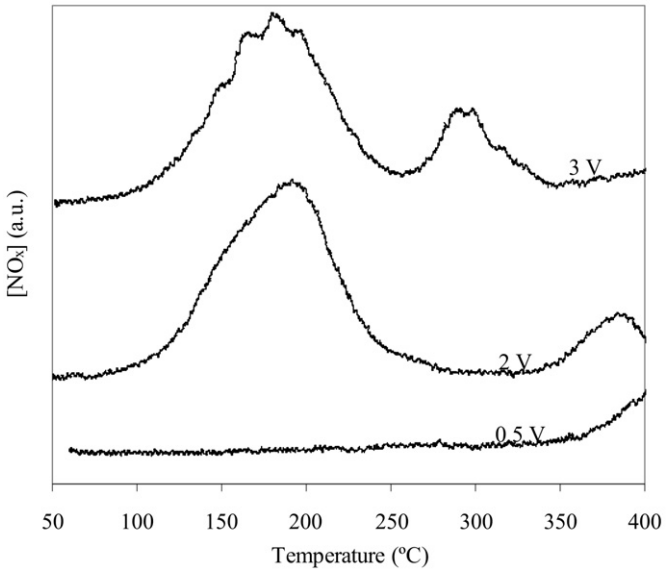

Fig. 12. NO_x desorption profile vs. temperature under application of different potentials: $V_{cell} = 0.5$, 2, 3 V. Adsorption conditions: $NO/C_3H_6/O_2$: 1000 ppm/1000 ppm/5%, 30 min of duration, $V_{cell} = -2$ V.

The presence of different potassium species on the catalyst surface also was detected by cyclic voltammetry. Fig. 13 shows the variation in the current along with the NO_x concentration versus a linear variation (5 mV s^{-1}) in the applied catalyst potential, between 3 and −2 V at 300 °C under a fixed lean composition (1000 ppm of NO, 1000 ppm of C_3H_6, 5% of O_2, He balance). As reported in previous studies with cationic conductor electrolytes [46,47], the observed cathodic and anodic peaks were directly linked to the back-spillover of ions between the solid electrolyte and the catalyst surface, leading to the electron charge-transfer reaction between the ions and the adsorbed species on the catalyst. During the cathodic scan, from 3 V to −2 V, three main cathodic peaks were observed, centred at −0.1 V, −1 V, and −1.5 V, which were attributed to the formation of different potassium species. According to the TPD measurements, the first peak centred at −0.1 V was attributed to the formation of a weak surface nitrate, whereas the second peak centred at −1 V was attributed to the formation of bulk potassium nitrate, due to greater interaction between potassium and NO_x (i.e., more negative potential). During the formation of both types of nitrates ($V_{cell} > -1$ V), the NO_x concentration was <1000 ppm; however, once the bulk potassium nitrates were completely formed at $V_{cell} < -1$ V, the NO_x concentration increased to 1000 ppm. The formation of such bulk alkali nitrates likely blocked

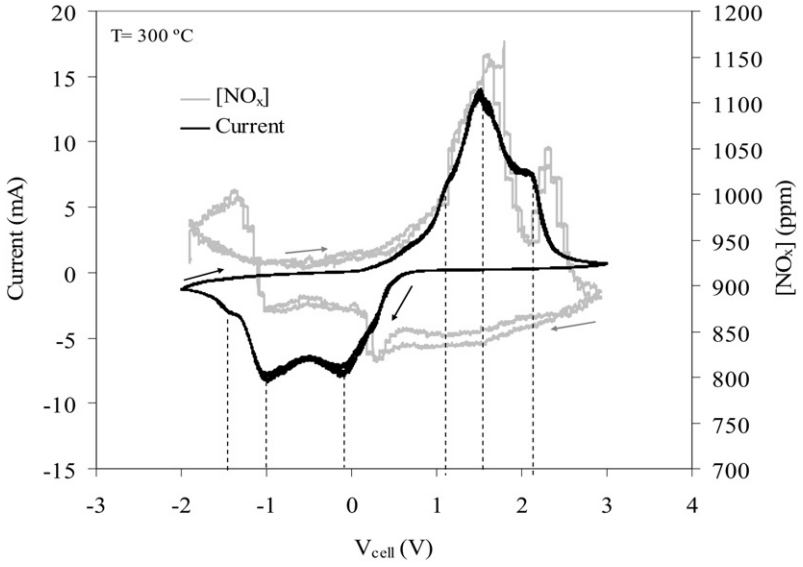

Fig. 13. Current and NO_x concentration variation vs. catalyst potential during cyclic voltammetry under lean reaction conditions at 300 °C. Scan rate: 5 mV s^{-1}.

most of the Pt sites, resulting in negligible SCR activity, as observed in previous experiments. On the other hand, the third cathodic peak at −1.5 V led to a further decrease in NO_x concentration, likely due to some SCR activity of the Pt catalyst. The greater amount of potassium transferred at this negative potential likely induced excessive coverage of O_2, with the subsequent formation of potassium oxide/peroxide phases, the origin of the observed cathodic peak at −1.5 V. Such species could have a promotional effect on SCR activity, with their formation leading to a decreased NO_x concentration. The presence of these species, marked by a cathodic voltammetry peak close to −2 V, also was observed in a previous study with Pt/K–βAl_2O_3 electrochemical catalyst, even at a lower O_2 concentration in the feed (1%) [22]. Thus, the three peaks observed during the cathodic polarization in cyclic voltammetry are in good agreement with the results shown in Figs. 5 and 6 where the influence of the negative polarization during the lean phase was studied. At low negative potentials, surface nitrates formed, leading to an insufficient storage capacity to saturate the Pt surface (cycles a and b in Fig. 5). But under more negative polarization, along with the formation of more surface nitrates, the formation of bulk potassium nitrate occurred, increasing the storage capacity of the catalyst (cycle c in Fig. 5) and blocking the Pt active sites (leading to a negligible final SCR activity). This assertion is in agreement with the proposed mechanism of formation of both nitrate species [48]. The formation of surface nitrate has been observed with a low alkali coverage of BaO in the Al_2O_3 sample, whereas the formation of bulk nitrate occurred for higher (20% BaO) alkali coverage in the Al_2O_3 sample, once a monolayer of surface nitrates was already formed [48]. On the other hand, during the anodic polarization from −2 to 3 V, the previously formed potassium species were decomposed, leading to three anodic polarization peaks centred at 1.1, 1.5, and 2.2 V. The first of these peaks was attributed to the decomposition of potassium oxide/peroxide phases. As mentioned earlier, these phases required a strong interaction of O_{ads} on the catalyst surface and therefore decomposed at moderate potentials (1.1 V). The decomposition of such species, which did not enclose a NO_x desorption peak to the gas phase, led to a small anodic peak with a similar shape of the corresponding formation peak at −1.5 V. The second anodic peak at 1.5 V was attributed to the decomposition of the surface nitrates weakly adsorbed on the catalyst surface, and the third peak at 2.2 V was attributed to the decomposition of the bulk potassium nitrates of greater stability. This assumption can be confirmed by examining the amount of NO_x released to the gas phase during the decomposition of each type of nitrate. More NO_x was released during the decomposition of the surface nitrate during the anodic peak at 1.5 V than during the decomposition of the bulk nitrate at 2.2 V, in good agreement with the TPD curves shown in Fig. 12.

Taking into account that both temperature and potential were the driving forces behind decomposition of the stored compounds, other parallels can be established between NO_x-TPD and cyclic voltammetry. A catalyst potential of 0.5 V was not sufficient to decompose the stored nitrates at 300 °C, as demonstrated by the cyclic voltammetry results, and higher temperatures were required, as evidenced by the TPD measurements. At 2.2 V, the surface nitrates were effectively decomposed at 300 °C, in agreement with the TPD spectra obtained under application of 2 V. Also at this potential (2.2 V), the bulk nitrates began to decompose at 300 °C in cyclic voltammetry, in agreement with the higher temperature (390 °C) required for the decomposition of these compounds during TPD at lower potential (2 V). Finally, a catalyst potential of 3 V was sufficient to decompose the bulk potassium nitrates during cyclic voltammetry, as confirmed by TPD measurements showing the maximum desorption temperature peak at 3 V of the bulk nitrates at around 300 °C. Thus, as confirmed by cyclic voltammetry, the application of 3 V was sufficient to completely regenerate the catalyst surface from storage compounds under lean conditions, allowing us to work under a fixed lean atmosphere, in good agreement with the results shown in Fig. 10. This can be further confirmed by the excellent reproducibility of the current curves for two different cycles in the voltammetry, which also agrees with the good reproducibility of the NO_x concentration profile. The range of reaction conditions investigated demonstrates the potential practical applications of this new electrochemically assisted NSR catalyst. In addition, the low applied potentials (3 and −2 V) used for trapping NO_x and regenerating the catalyst surface will help maximize the operational life of the electrochemical cell.

4. Conclusion

In this work, numerous findings were revealed as a result of coupling catalysis and solid-state electrochemistry for the electrochemically assisted NSR catalyst. Using an electrochemical catalyst in which the ions electrochemically transferred from the support can effectively act as a storage component (e.g., potassium ions) opens up a new range of alternatives not only for fundamental studies, but also for technological advancement of the NSR process. The main conclusions of this work can be summarized as follows:

- Using a solid electrolyte cell in the NSR process allows monitoring of the lean and regeneration periods by measuring the current generated during the applied potential in each phase. This can facilitate optimisation of the duration of both sequences at each reaction condition in a technically feasible manner.
- Potassium ions electrochemically transferred to the Pt catalyst play a double role in the NSR process, as a promoter for the NO oxidation reaction and as storage sites through the formation of potassium nitrates. Thus, moderated values of the negative polarization in the lean phase should be applied to balance both functions.
- The maximum yield of the Pt/K–βAl_2O_3 to effectively reduce NO_x to N_2 was obtained at 300 °C. However, the possibility of controlling the stability of the stored nitrates by varying the value of the applied catalyst potential during the regeneration phase would probably allow improvement of the system's efficiency under other reaction conditions as well.
- The ability of the electrochemical catalyst to work under wet conditions demonstrates the potential practical uses of this novel system. In addition, the possibility of electrochemically regenerating the catalyst surface (without switching the gas atmosphere to a rich environment) implies an important technological advance that can simplify the current NSR technology.
- NO_x-TPD and cyclic voltammetry measurements confirmed the foregoing conclusions and revealed the presence of two different types of potassium nitrates electrochemically trapped on the catalyst surface, a weakly adsorbed surface nitrate and a strongly adsorbed bulk potassium nitrate.

Acknowledgments

Financial support by the Ministerio de Educación y Ciencia of Spain (projects CTQ2004-07350-C02-01/PQ and CTQ2007-62512/PPQ) and the European Marie-Curie EFEPOC Project (MSCF-CT-2006-046201) are gratefully acknowledged.

References

[1] K.M. Adams, J.V. Cavataio, R.H. Hammerle, Appl. Catal. B 10 (1996) 157.
[2] A. Kotsifa, D.I. Kondarides, X.E. Verykios, Appl. Catal. B 72 (2007) 136.
[3] S. Hammache, L.R. Evans, E.N. Coker, J.E. Miller, Appl. Catal. B 78 (2008) 315.
[4] L. Lietti, P. Forzatti, I. Nova, E. Tronconi, J. Catal. 204 (2001) 175.

[5] L. Campbell, R. Dazinger, E. Guth, S. Padron, US Patent 5 451 558 (1994) to Goal Line Environmental Technologies.
[6] N. Takahashi, H. Shinjoh, T. Ijima, T. Suzuki, K. Yamazaki, K. Yokota, H. Suzuki, N. Miyoshi, S.-I. Matsumoto, T. Tanizawa, T. Tanaka, S.S. Taeishi, K. Kasahara, Catal. Today 27 (1996) 63.
[7] S. Matsumoto, Catal. Today 29 (1996) 43.
[8] H. Shinjoh, N. Takahashi, K. Yokota, M. Sugiura, Appl. Catal. B 15 (1998) 189.
[9] M. Konsolakis, I.V. Yentekakis, Appl. Catal. B 29 (2001) 103.
[10] L.G. Neal, J.L. Haslbeck, H. Tseng, US patent 4 755 499 (1988) to Noxso Corporation.
[11] L.J. Gill, P.G. Blakeman, M.V. Twigg, A.P. Walter, Top. Catal. 28 (2004) 157.
[12] T.J. Toops, D.B. Smith, W.P. Partridge, Appl. Catal. B 58 (2005) 245.
[13] T.J. Toops, D.B. Smith, W.S. Epling, J.E. Parks, W.P. Partridge, Appl. Catal. B 58 (2005) 255.
[14] T.J. Toops, D.B. Smith, W.P. Partridge, Catal. Today 114 (2006) 112.
[15] M. Stoukides, C.G. Vayenas, J. Catal. 70 (1981) 137.
[16] C.G. Vayenas, S. Bebelis, S. Ladas, Nature (London) 343 (1990) 625.
[17] C.G. Vayenas, S. Bebelis, I.V. Yentekakis, H.-G. Lintz, Catal. Today 11 (1992) 303.
[18] I.V. Yentekakis, G. Moggridge, C.G. Vayenas, R.M. Lambert, J. Catal. 146 (1994) 293.
[19] X. Li, P. Vernoux, Appl. Catal. B 61 (2005) 267.
[20] N. MacLeod, F.J. Williams, M.S. Tikhov, R.M. Lambert, Angew. Chem. Int. Ed. 44 (2005) 3730.
[21] S. Ladas, S. Bebelis, C.G. Vayenas, Surf. Sci. 251 (1991) 1062.
[22] A. de Lucas-Consuegra, F. Dorado, J.L. Valverde, R. Karoum, P. Vernoux, J. Catal. 251 (2007) 474.
[23] A. de Lucas-Consuegra, F. Dorado, C. Jimenez-Borja, J.L. Valverde, Appl. Catal. B 78 (2008) 222.
[24] F. Dorado, A. de Lucas-Consuegra, P. Vernoux, J.L. Valverde, Appl. Catal. B 73 (2007) 42.
[25] F. Dorado, A. de Lucas-Consuegra, C. Jiménez, J.L. Valverde, Appl. Catal. A 321 (2007) 86.
[26] F.J. Williams, A. Palermo, S. Tracey, M.S. Tikhov, R.M. Lambert, J. Phys. Chem. B 106 (2002) 5668.
[27] F.J. Williams, M.S. Tikhov, A. Palermo, N. MacLeod, R.M. Lambert, J. Phys. Chem. B 105 (2001) 2800.
[28] C.M.L. Scholz, V.R. Gangwal, J.H.B.J. Hoebink, J.C. Schouten, Appl. Catal. B 70 (2007) 226.
[29] K. Yamazaki, N. Takahashi, H. Shinjoh, M. Sugiura, Appl. Catal. B 53 (2004) 1.
[30] F.A. Cotton, G. Wilkinson, Advanced Inorganic Chemistry, fifth ed., Wiley, New York, 1988.
[31] W. Epling, L. Campbell, A. Yezerets, N. Currier, J. Parks, Catal. Rev. 46 (2004) 163.
[32] W.S. Epling, A. Yezerets, N.W. Currier, Appl. Catal. B 74 (2007) 117.
[33] S.S. Mulla, N. Chen, L. Cumaranatunge, W.N. Delgass, W.S. Epling, F.H. Ribeiro, Catal. Today 114 (2006) 57.
[34] S.S. Mulla, N. Chen, W.N. Delgass, W.S. Eppling, F.H. Ribeiro, Catal. Lett. 100 (2005) 267.
[35] J. Xiao, X. Li, S. Deng, F. Wang, L. Wang, Catal. Commun. 9 (2007) 563.
[36] L. Castoldi, I. Nova, L. Lietti, P. Forzatti, Catal. Today 96 (2004) 43.
[37] B.W. Krupay, Y. Amenomiya, J. Catal. 76 (1982) 345.
[38] M. Kantschewa, E.V. Albano, G. Ertl, H. Knozinger, Appl. Catal. 8 (1983) 71.
[39] E. Fridell, M. Skoglundh, B. Westerberg, S. Johansson, G. Smedler, J. Catal. 183 (1999) 196.
[40] A. Lindholm, N.W. Currier, E. Fridell, A. Yezerets, L. Olsson, Appl. Catal. B 75 (2007) 78.
[41] W.S. Epling, J.E. Parks, G.C. Campbell, A. Yezerets, N.W. Currier, L.E. Campbell, Catal. Today 96 (2004) 21.
[42] A. Amberntsson, H. Persson, P. Engstrom, B. Kasemo, Appl. Catal. B 31 (2001) 27.
[43] W.S. Epling, D. Kisinger, C. Everest, Catal. Today 136 (2008) 156.
[44] J.H. Kwak, D.H. Kim, T. Szailer, C.H.F. Peden, J. Szanyi, Catal. Lett. 111 (2006) 119.
[45] C. Verrier, J.H. Kwak, D.H. Kim, C.H.F. Peden, J. Szanyi, Catal. Today 136 (2008) 121.
[46] A. de Lucas-Consuegra, F. Dorado, J.L. Valverde, R. Karoum, P. Vernoux, Catal. Commun. 9 (2008) 17.
[47] P. Vernoux, F. Gaillard, C. Lopez, E. Siebert, Solid State Ionics 175 (2004) 609.
[48] J. Szanyi, J.H. Kwak, D.H. Kim, S.D. Burton, C.H.F. Peden, J. Phys. Chem. B Lett. 109 (2005) 27.